energies

Article

Verification of the Discrete Ordinates Goal-Oriented Multi-Collision Source Algorithm with Neutron Streaming Problems

Xinyu Wang [1], Bin Zhang [1,*], Yixue Chen [1] and Jun Xiong [2]

[1] School of Nuclear Science and Engineering, North China Electric Power University, Beijing 102206, China
[2] State Key Laboratory of Nuclear Power Safety Monitoring Technology and Equipment, Shenzhen 518172, China
* Correspondence: zhangbin@ncepu.edu.cn

Abstract: The shielding calculation of neutron streaming problems with ducts is characterized by the strong anisotropy of angular flux, which poses a challenge for the analysis of nuclear installations. The discrete ordinate method is one of the most commonly deterministic techniques to solve the neutron transport equation, in which the accuracy and efficiency neutron are crucial to ensure the reliability of the streaming shielding simulation. We implemented the goal-oriented multi-collision source algorithm in the 3D transport code ARES. This algorithm can determine the importance factor based on the adjoint transport calculation, obtain the response function to enable problem-dependent, goal-oriented spatial decomposition, and provide the error estimation as a driving force behind the dynamic quadrature to optimize the source iteration. This study focuses on verifying the goal-oriented multi-collision source algorithm under the neutron streaming problems, and the capabilities of the algorithm have been tested on IRI-TUB benchmark of SINBAD database. The numerical results show that the algorithm can effectively control the angular discretization error for the neutron streaming problems, which is more economical than the traditional discrete ordinate calculation.

Keywords: shielding calculation; neutron streaming; discrete ordinates method; multi-collision source; goal-oriented

Citation: Wang, X.; Zhang, B.; Chen, Y.; Xiong, J. Verification of the Discrete Ordinates Goal-Oriented Multi-Collision Source Algorithm with Neutron Streaming Problems. *Energies* **2022**, *15*, 8335. https://doi.org/10.3390/en15228335

Academic Editors: Shichang Liu, Jingang Liang and Zhaoyuan Liu

Received: 15 October 2022
Accepted: 6 November 2022
Published: 8 November 2022

1. Introduction

Accurate shielding calculations are the basis for the analysis of nuclear installations; at the core is the solution of the neutron transport equation. The discrete ordinate method (S_N) is one of the primary methods for solving the equation, which discretizes the continuous angle variable by defining a discrete quadrature set in the angle space [1]. However, the quadrature sets without arbitrary rotation invariance lead to inevitable discretization errors into the angular discrete approximation, which are the so-called ray effects [2]. The neutron streaming problems with ducts or narrow gaps have more significant ray effects in particular, because of the serious anisotropy of angular flux [3]. In actual neutron streaming shielding calculations, it is very important to mitigate the discretization errors and achieve balance between the accuracy and efficiency of transport calculation to ensure the reliability of shielding calculations [4].

Several techniques for mitigating the angular discretization errors have been proposed in most shielding calculation codes based on the discrete ordinate method [5]. AMTRAN, a neutron and gamma transport code developed at Lawrence Livermore National Laboratory, uses angular adaptive refinement for increasing the discrete directions of quadrature sets in a region with angular flux anisotropy to improve the numerical integration precision [6]. Longoni and Haghighat investigated the ordinate splitting method (OS) [7] and regional angle refinement method (RAR) [8] and implemented the algorithms into the three-dimensional particle transport code PENTRAN [9]. The collision source method is another widely used in discretization error mitigation, which calculates the uncollided and collided fluxes using a high-order transport or analytical method [10]. Oak Ridge National Laboratory developed GTRUNCL and FNSUNCL3 modules upon the first collision source method and applied them to the transport system DOORS [11,12]. Some other well-known codes on the basis of the first collision source method are DENOVO [13], IDT of CEA [14], and AETIUS of KAERI [15].

In previous studies, we developed the goal-oriented multi-collision source method (GO-MCS) according to the multi-dimensional discrete ordinates transport code ARES [16]. The GO-MCS method is the expansion and extension of the first collision source method, which not only concerns the uncollision flux, but also the calculation of collided fluxes via spatial decomposition for solving the Boltzmann equation in transport problems with anisotropy [17]. The GO-MCS method is composed of both goal-oriented spatial decomposition and dynamic quadrature. The former can adaptively determine a problem-dependent, goal-oriented spatial decomposition in accordance with the importance factor based on the adjoint transport calculation, while the difference in the scalar fluxes from one high-order quadrature set to a lower one provides the error estimation as a driving force behind the dynamically changing the angular quadrature in remaining iterations.

Nevertheless, this method is only used to solve simple one-group models, and there is no precedent to solve multiple sets of complex practical transport problems. In addition, in actual nuclear reactors, when neutrons collide with the atomic nucleus in the thermal groups, they may obtain energy for the up-scattering [18]. Therefore, additional up-scattering iterations should be performed in the source iteration. After the iteration process among the whole groups, the thermal groups should be cycled through until they have converged on up-scattering [19]. The above issues need to be studied to expand the usage scenarios of the method.

This study concentrates on the verification of the algorithm's capabilities for solving the neutron streaming problems by means of the IRI-TUB benchmark and also focuses on the up-scattering effect of neutrons in thermal groups. Numerical results from the method are compared against the results obtained with the standard ARES code. An overview of the GO-MCS method is briefly presented in Section 2, followed by the implementation of the thermal iteration in Section 3. Section 4 contains the description, numerical results and discussion of the IRI-TUB Benchmark. In this section, it should be noted that the setting of calculation parameters is estimated in relation to a self-designed simplified model in line with the benchmark. Finally, the conclusions and suggestions for further research are summarized in Section 5.

2. Goal-Oriented Multi-Collision Source Algorithm

2.1. Multi-Collision Source Calculation

For simplicity, the steady-state neutron transport equation without a fission source term can be written in operator form

$$\boldsymbol{L}\psi^{(n)} = \boldsymbol{S}\psi^{(n-1)} + Q \tag{1}$$

where ψ is the angular flux after iteration n, $\boldsymbol{L}$ is the streaming-collision operator, $\boldsymbol{S}$ is scattering operator and Q is the source term. If the initial scattering source is estimated to be zero, the source iteration angular flux estimate after n sweeps is, physically, the angular flux due to particles that have experienced at most $n-1$ scattering events.

The multi-collision source method divides the entire model space into two parts (marked as A and B) when calculating the collided fluxes. The scattering source ($\boldsymbol{S}\psi^{(n-1)}$) can be defined as the sum of the scattering sources (Q_A and Q_B) of the two parts. The angular fluxes that are scattered in regions A and B are now defined as $\boldsymbol{L}^{-1}Q_A$ and $\boldsymbol{L}^{-1}Q_B$, which can be calculated with high-order and low-order quadrature sets for transport sweeping, respectively. As mentioned above, the flux after iteration n can be calculated from

$$\psi_{MCS}^{(n)} = \boldsymbol{L}^{-1}Q_A + \boldsymbol{L}^{-1}Q_B \tag{2}$$

and the iteration equation is given by

$$\boldsymbol{L}\psi_{MCS}^{(n+1)} = \boldsymbol{S}\psi_{MCS}^{(n)}(n \to \infty) \tag{3}$$

After a sufficient number of iterations, both sides of the equation will converge to within some given tolerance, and the total angular flux is given by

$$\psi = \sum_{n=0}^{\infty} \psi_{MCS}^{(n)} \tag{4}$$

2.2. Goal-Oriented Spatial Decomposition

The spatial decomposition of GO-MCS method is related to the physical characteristics of the transport problem. For neutron streaming problems, people show more concern to an accurate detector response in ducts or narrow gaps than an exact solution across the whole model. The goal-oriented algorithm plays an important part for the accurate detector response with as small a computation amount as possible. This spatial decomposition scheme can ensure the use of high-order quadrature sets in anisotropy regions (such as ducts). Considering the anisotropy of angular fluxes in high-energy groups, the judgement of spatial decomposition only needs to be carried out in the highest energy group for multi group problems. The spatial decomposition scheme generated in the highest energy group can also be effectively applied in other energy groups.

The neutron importance function is expressed by the solution of the adjoint transport equation

$$-\boldsymbol{\Omega} \cdot \nabla\psi^* + \Sigma_t\psi^* = \int_{\boldsymbol{\Omega}'} \Sigma_s\left(\boldsymbol{\Omega} \to \boldsymbol{\Omega}'\right)\psi^* d\boldsymbol{\Omega}' + Q^* \tag{5}$$

where ψ^* is the adjoint angular flux, Q^* is the adjoint source. The larger the adjoint angular flux is, the greater the probability that neutrons in this direction at this position in phase space will be detected. The adjoint scalar flux was used to estimate the neutron importance in this study, as $\phi^* = \int_{4\pi} \psi^* d\boldsymbol{\Omega}$. The adjoint transport equation only shows the relative contribution of different positions to the detector response, but does not contemplate the contribution of forward transport calculation. Based on the contribution theory [20], the optimized scalar contribution flux is defined as the product of the forward and adjoint angular fluxes, and the normalized contribution factor C in the spatial domain D is defined as

$$C(r) = \frac{\phi(r) \cdot \phi^*(r)}{\int_D dr\phi(r) \cdot \phi^*(r)} \tag{6}$$

The contribution factor introduces the forward solution as the weight coefficient and directs the model's significance function to be more acceptable. It takes into account all contributions of forward solution and adjoint solution, which makes it a more suitable significance function for spatial decomposition than neutron importance. The contribution factor in the GO-MCS method operates on the problem domain in two distinct parts: the colliding fluxes calculation component ($A = \{r|C(r) > \Delta C\}$) and the remainder part ($B = D - A$), where ΔC is a user-defined tolerance.

2.3. Dynamic Quadrature Technique

Assuming that the angular flux becomes gradually smooth with the number of iterations, the dynamic quadrature technique adaptively reduces the order of the quadrature set in remaining iterations after multi-collision source calculation. Two error sources of the error produced should be concerned in changing the quadrature set in a certain iteration: the relative quadrature error (ε_q) and the relative iterative error (ε_i). Hence, the total relative error (E_{tot}) is defined as

$$E_{\text{tot}} \leq \varepsilon_q \cdot \varepsilon_i < \Delta E, \tag{7}$$

where ΔE is a user-defined error convergence criterion. To estimate the error introduced by the alteration of quadrature sets, we performed an extra transport sweep with a lower-order quadrature set after completing one iteration and compared the current iteration scalar flux ($\phi^{(n),N}$) with the extra calculation scalar flux ($\phi^{(n),N'}$). The relative quadrature error can be estimated as

$$\varepsilon_q = \frac{\phi^{(n),N'} - \phi^{(n),N}}{\phi^{(n),N}} \tag{8}$$

When changing the quadrature set from order N to N' in a certain iteration, E_{tot} can be calculated as

$$E_{\text{tot}} \le \varepsilon_q \cdot \frac{\phi_t^{(\infty),N} - \phi_t^{(n),N}}{\phi_t^{(\infty),N}}, \tag{9}$$

where $\phi_t^{(n),N}$ is the total scalar flux after n sweeps with the Nth order quadrature set. The second term on the right side of Equation (9) is the iteration relative error (ε_i). Due to the source iteration of the linear Boltzmann equation exhibiting monotonic convergence, the iteration relative error can be obtained by estimating the spectral radius (σ):

$$\frac{\phi_t^{(\infty)} - \phi_t^{(n)}}{\phi_t^{(\infty)}} \le \frac{\phi_t^{(\infty)} - \phi_t^{(n)}}{\phi_t^{(n)}} = \varepsilon_i = \frac{\sigma}{1-\sigma}\frac{\phi^{(n)}}{\phi_t^{(n)}} \tag{10}$$

3. Implementation of Thermal Iteration

Neutron thermalization refers to the process through which neutrons slow down in thermal groups. Due to the fact that the kinetic energy of the neutrons in the thermal groups is similar to that of the thermal motion of the medium atomic nucleus, these neutrons have the potential to scatter to a lower energy group while also scattering to a higher energy group in the process of scattering collisions. Only the thermal groups with energies lower than about 0.4 eV exhibit enough up-scattering to justify thermal iteration cycles; therefore, we need to carry out more thermal iterations within this energy range. Figure 1 displays a simplified flowchart of this procedure.

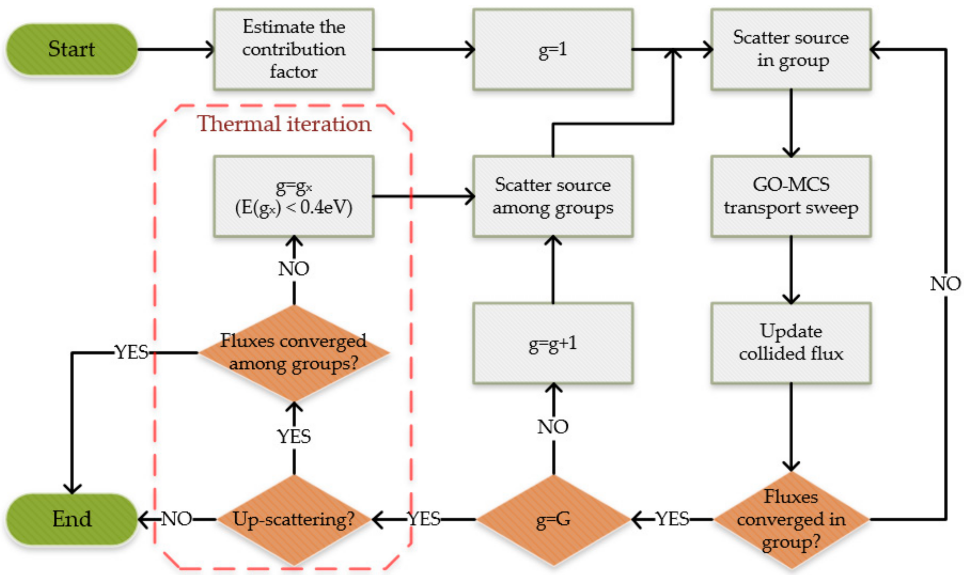

Figure 1. Flowchart of iteration for the GO-MCS method.

This iterative process is not the traditional source iteration approach which is often used. During the pre-processing stage, the forward and adjoint fluxes need to be solved independently in order to accurately estimate the contribution factor. This step comes before the source iteration. In addition, we break down the overall flux in one group into the fluxes that come from the various collision sources and compute those fluxes individually. The thermal iteration begins with the group g_x, whose energy $E(g_x)$ is less than 0.4 eV. This is the starting point for thermal groups. After there has been convergence in the groups that are above the thermal range, this should drive the thermal iteration closer to reaching complete convergence.

4. Results and Discussion

In handling complicated practical shielding issues, direct computation without prediction is not a good option. For applying the GO-MCS method to the IRI-TUB benchmark, simulation efficiency and precision are jointly determined by the production of contribution factor, quadrature sequence of dynamic quadrature, and model characteristics. To study these elements of neutron streaming shielding computation, we created a simple model based on the IRI-TUB benchmark and used the simplified model's transport calculation to inform the establishment of calculation parameters for the IRI-TUB benchmark calculation.

4.1. Self-Designed Simplified Model

The self-designed simplified model is a rectangular block made of a half-scattering material containing a straight duct, whose size is approximate to the IRI-TUB benchmark. The dimensions of the geometric model are 50 cm × 200 cm × 50 cm, as shown in Figure 2. Reflective boundary conditions are adopted for the boundary planes x = 0 and z = 0, and vacuum boundary conditions at other boundaries. The material source strengths and cross-sections are given in Table 1.

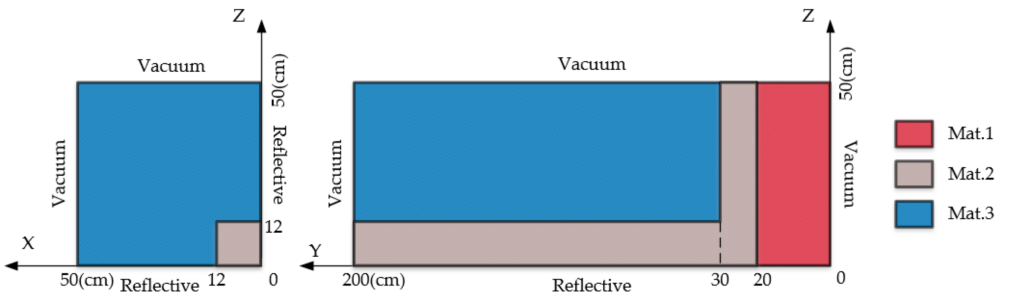

Figure 2. Geometry of the self-designed neutron streaming problem.

Table 1. Source strength and cross-sections of the self-designed neutron streaming problem.

Materials	Source ($n \cdot cm^{-3} \cdot s^{-1}$)	Total Cross-Section (cm^{-1})	Scattering Cross-Section (cm^{-1})
Mat.1	1	0.1	0.05
Mat.2	0	10^{-4}	0.5×10^{-4}
Mat.3	0	0.1	0.05

The mesh used for calculation was composed of 25 × 100 × 25 Cartesian grids with a mesh resolution of 2 cm, as shown in Figure 3. The source region was a plate with a thickness of 20 cm, and there was a 10 cm gap between the source and the shield. This problem exhibited a void duct with a length of 170 cm in the neutron shield, which is a typical neutron streaming problem. The spatial discretization scheme was directional theta-weighted (DTW) with an iterative convergence criterion of 10^{-4}. The simulation of this issue used the S_{100} order Legendre–Chebyshev quadrature set ($P_N T_N$) with 10,200 directions is utilized as the reference solution. Seventeen key points were uniformly distributed along the duct from the entrance with an interval of 10 cm, and the neutron fluxes at the key points were used for comparison and analysis.

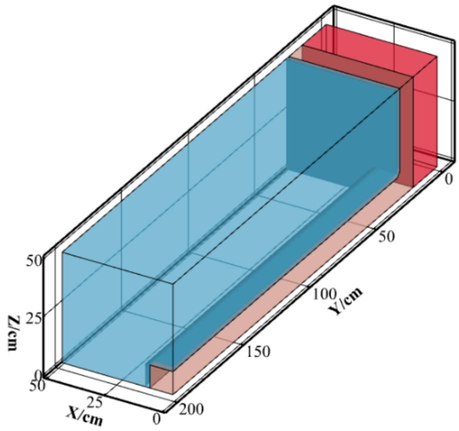

Figure 3. Computational model of the self-designed neutron streaming problem.

Prior to the transport procedure for the GO-MCS calculation, it is important to determine the contribution factor for goal-oriented spatial decomposition. Both the forward and adjoint transport calculations for the contribution factor are performed in the same computational model. Due to the estimation's lack of a requirement for exceedingly exact findings, these calculations are carried out utilizing the S_{32}-order P_NT_N quadrature set (5040 directions). The macro section of the material is employed as the adjoint source term, and the duct outlet is used as the adjoint source region for adjoint calculations. Figure 4a depicts the distribution of the contribution function. It is not required to obtain precise reaction rate calculation results because the conjugate neutron flux density simply has to offer the spatial associated particle relative significance distribution to direct the next spatial decomposition. In this problem, the spatial decomposition used a user-defined tolerance ΔC of 1×10^{-5}. With this tolerance, the spatial decomposition is shown in Figure 4b.

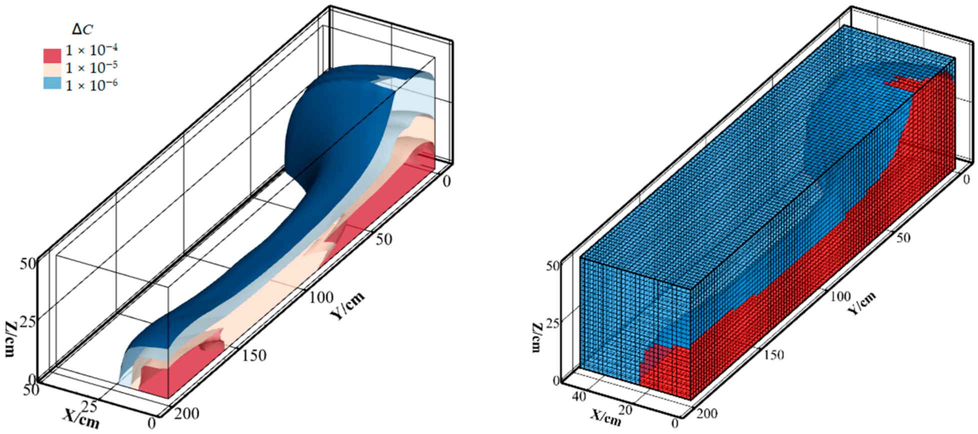

(**a**) (**b**)

Figure 4. Spatial decomposition of the neutron streaming shielding problem. (**a**) The distribution of the contribution function; (**b**) the spatial decomposition with tolerance $\Delta C = 1 \times 10^{-5}$.

The traditional approach for solving the S_N equation employs P_NT_N quadrature sets with orders of S_{32}, S_{40}, and S_{60}. The GO-MCS calculation is divided into two sections: the collision source part, which uses a combination of S_{32}- and S_{100}-order P_NT_N quadrature sets to calculate the uncollided and the first uncollided fluxes; the dynamic quadrature part, which uses a smooth quadrature sequence including four P_NT_N quadrature sets ($S_{16}/S_{32}/S_{40}/S_{60}$) to ensure a smooth transition from more to less angular discretization directions as much as possible, and the effect of quadrature set calls on the computational results is observed by varying the user-defined adaptive iterative convergence criterion (ΔE). Figure 5 displays the relative errors that exist between the two different types of computation results and the reference solution. As the distance between the key points and the entrance of the duct increases, the relative errors of the traditional S_N calculations show large fluctuations related to the order of quadrature sets, and the relative errors of some key points exceed 20%. The ray effects may account for the apparent discrepancies between traditional S_N results. Due to ray effects, even the S_{60} approach produces significant inaccuracies for this problem. Despite this, the relative errors of the computed results with respect to the reference solution in the range of 30 cm to 100 cm do not surpass 1% under any of the situations. On the other hand, the angular discretization error is effectively managed; the global maximum relative error value produced by the GO-MCS calculation is just 3.56%.

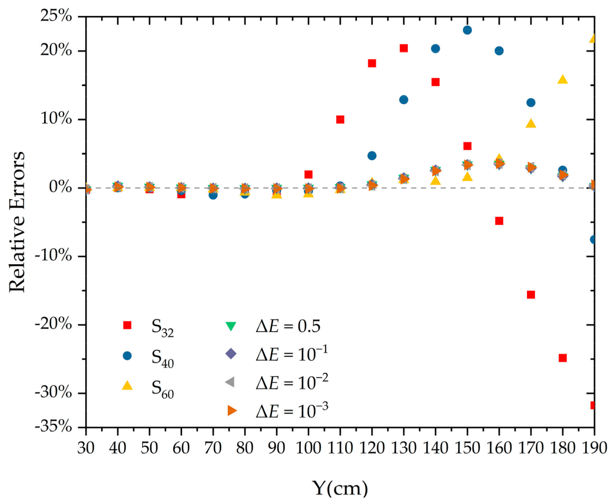

Figure 5. Relative errors of key points for the neutron streaming shielding problem.

The adaptive iterative convergence criteria (ΔE) in the reduced-order component of the quadrature sets are strongly associated with the efficiency of the GO-MCS method, because it directly influences the number of calls to various quadrature sets in the quadrature sequence. For a particular quadrature sequence, the computation time is proportional to the number of iterations required to invoke the higher-order quadrature set. Figure 6 depicts the invocations of five distinct quadrature sets (including the S_{100}-order quadrature set invoked for the collided flux calculations) when the convergence criterion is changed from 0.5 to 0.001, and as ΔE decreases, the number of invocations of higher-order quadrature sets significantly increases and the computation time increases. The phenomena in which the order of the quadrature set drops with each iteration are also compatible with the prior assumption that the scattering process tends to smooth out the angular flux.

The root mean square of relative errors, also known as E_{RMS}, was determined for the scalar flux as a measure of error. This was performed in comparison to the reference results, which can be calculated as follows

$$E_{RMS} = \sqrt{\frac{1}{M}\sum_{m=1}^{M}\left(\frac{\phi_m - \phi_{m,ref}}{\phi_{m,ref}}\right)^2} \tag{11}$$

where m is the spatial index, M is the total number of spatial elements, ϕ_m is the calculated scalar flux, and $\phi_{m,ref}$ is the scalar flux of the reference results. Figure 7 displays the results of a comparison of the accuracy and efficiency of calculations performed under a variety of different settings. The accuracy of the GO-MCS calculation for this neutron flow problem is noticeably higher than that of the S_{60}-order quadrature set, and the calculation time is only 1.42 to 1.88 times as long; however, the acceleration ratio is 1.77 to 2.35 when compared with the calculation time required to obtain the reference solutions. Along with the drop in ΔE, there is also a modest reduction in E_{RMS}, but the overall computation time has greatly increased. It is possible that increasing the number of calls made by higher-order quadrature sets would enhance the calculation accuracy, but it will also increase the amount of time required to perform the computation. The GO-MCS technique is able to suitably organize the call sequence of quadrature groups in order to establish a reasonable balance between the accuracy of the calculations and the efficiency of the calculations.

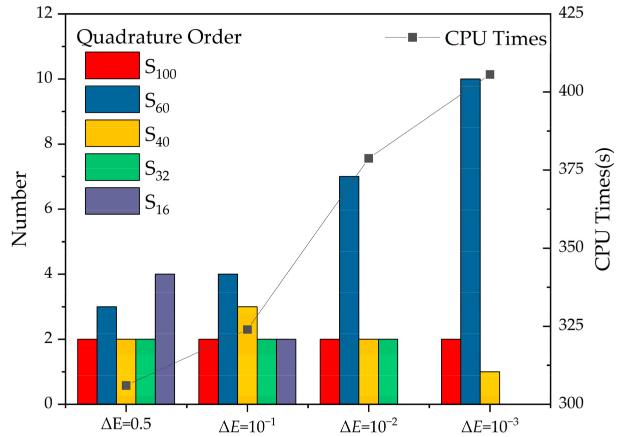

Figure 6. Effect of the tolerance criterion (ΔE) on the number of times the quadrature is used and the efficiency.

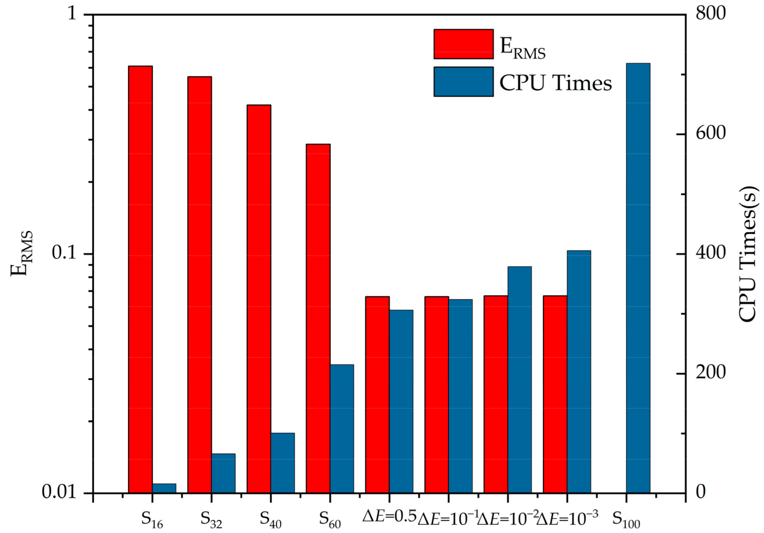

Figure 7. Comparison of accuracy and efficiency with different calculation schemes.

4.2. IRI-TUB Benchmark

The IRI-TUB research reactor, which is located in the Nuclear Technology Department of the Technical University of Budapest, is used to research the transport of fast and thermal neutrons via a duct [21]. Figure 8 demonstrates the geometric model. The reactor comprises a core and a huge radiation duct. In the active region, there is an asymmetrical arrangement of 24 fuel rods, each of which measures 7.2 cm by 97.2 cm. The reflecting layer, which is composed of graphite and water, is located around the core, while the aluminum shield is located outside the core. Inside the concrete block is an 11.8 cm inner diameter straight duct that faces the core. The length of the duct is 187 cm, and its wall is composed of stainless steel with a thickness of 0.45 cm. Five detectors were set up along the duct axis at distances of 0 cm, 67 cm, 121 cm, 148 cm, and 175 cm from the entrance of the duct. The accuracy of the numerical calculation of the fast neutron flux above 1 MeV was evaluated by measuring the ^{115}In(n, n′)^{115m}In reactive rate. In addition, measured neutron spectra in the straight duct at the entrance and at the fourth position are given for reference. This issue is characterized by highly anisotropic fluxes across the duct and up-scattering of thermal neutrons due to the presence of ^{12}C in graphite and ^{1}H in water near the core. This particular issue presents a challenging obstacle for angular discretization and iterative processes using the S_N method; thus, the purpose of this problem is to illustrate the capability of the GO-MCS method to solve to complex multi-group issues of straight ducts in the presence of up-scattering.

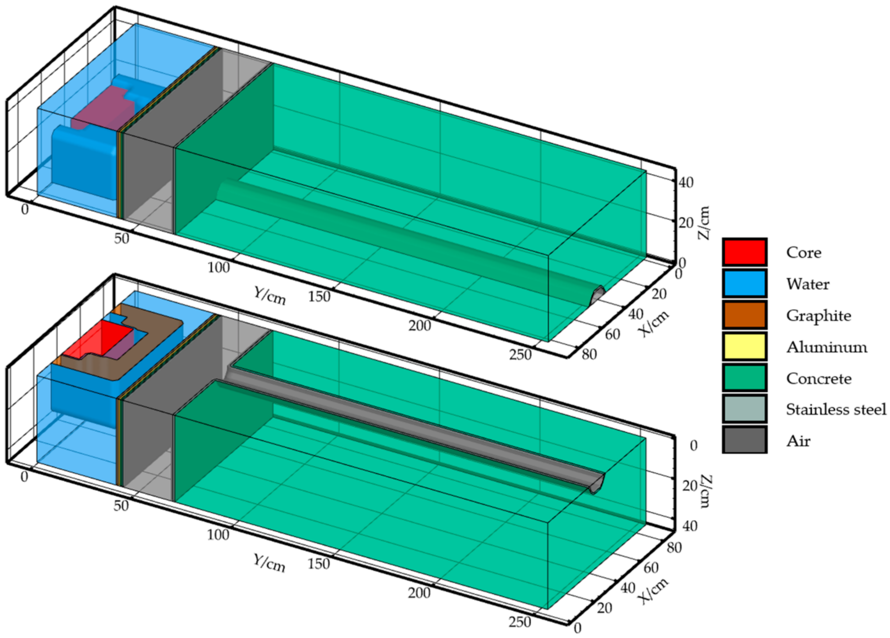

Figure 8. Geometry of the IRI-TUB benchmark problem.

The mesh used for all calculations was built from 45 × 153 × 45 cartesian grids using the DTW discretization scheme with an iterative convergence criterion of 10^{-4}. Reflective boundary conditions were adopted for the boundary planes z = 0, and vacuum boundary conditions at other boundaries. The issue was solved using third-order (P_3) scattering along with a 199-group structure for energy discretization. The multigroup cross-section library KASHIL-E70 [22] was used to obtain the cross-section messages. Figure 9 depicts the distribution of the contribution function. The adjoint source area was positioned near the duct outlet, and the model employed the spatial decomposition scheme generated at $\Delta C = 1\times10^{-3}$. For the dynamic quadrature algorithm, a sequence ($S_8/S_{16}/S_{32}/S_{40}/S_{60}$) was used in the GO-MCS calculation. The number of collisions set by GO-MCS was 1, meaning that the method calculated the uncollided flux and the first-collided flux with a high-order quadrature set (S_{100}-order combined with S_{32}-order $P_N T_N$, S_{100}-S_{32}).

To describe the neutron motion in thermal groups, different scattering nucleus models were used to approximate the treatment for different scattering materials. For example, the Nelkin scheme is generally used for ^{1}H in water [23]; the Parks D.E scheme is generally chosen for ^{12}C in graphite [24]. The energy groups that fall below 0.4 eV are classified as thermal groups, and there are a total of 19 thermal groups in the 199-group structure (from 3.67×10^{-1} eV to 1.00×10^{-5} eV).

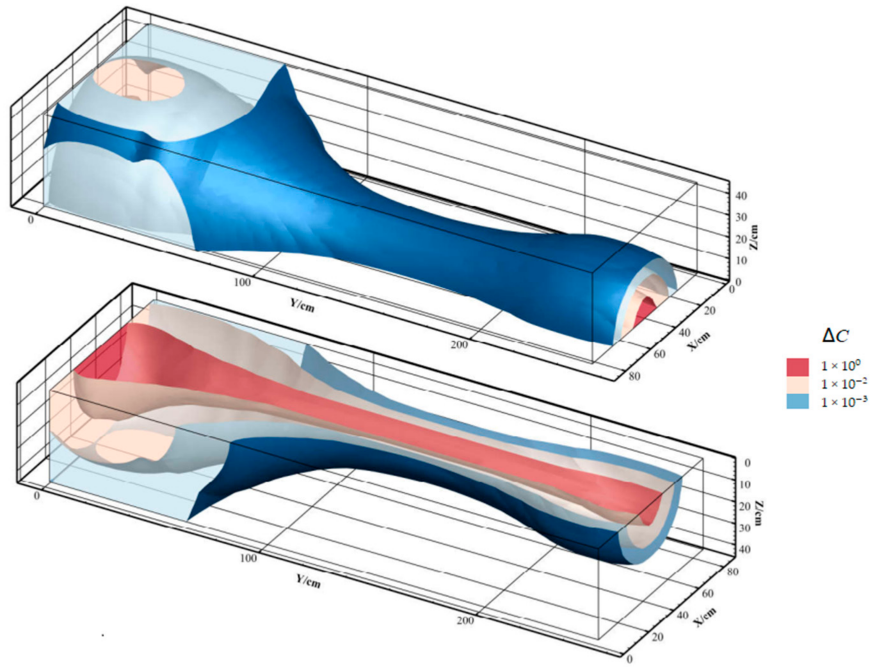

Figure 9. The contribution factor distribution for the IRI-TUB benchmark.

The actual reaction rates and the calculated response rates for each of the five straight orifice positions are compared in Table 2, including the results of the ARES code's direct 3D particle transport calculation with S_{60}-order $P_N T_N$ quadrature set and the GO-MCS calculation. The comparison in Table 1 demonstrates that the results of GO-MCS method are more consistent with the measured results than the traditional S_N solution. Near the duct outlet, the relative error of the $P_N T_N$-S_{60} quadrature set between the predicted result and measurement is within 17%. As the distance from the duct intake rises, the angular flux often exhibits a high degree of anisotropy. Despite having 3720 directions, the S_{60}-order $P_N T_N$ quadrature set is incapable of achieving the required resolution to precisely characterize the angular flux down the duct. However, the relative error of the GO-MCS calculation near the duct outlet is only approximately 10%.

Table 2. Calculated and measured values of ^{115}In(n, n′)^{115m}In reactive rate.

Distances from Entrance (cm)	Measured (s^{-1})	$P_N T_N$-S_{60} (s^{-1})	GO-MCS (s^{-1})
0	5.57×10^{-16}	5.39×10^{-16}	5.61×10^{-16}
67	3.17×10^{-17}	2.98×10^{-17}	3.14×10^{-17}
121	7.70×10^{-18}	8.87×10^{-18}	8.10×10^{-18}
148	4.61×10^{-18}	5.20×10^{-18}	4.97×10^{-18}
175	3.01×10^{-18}	3.52×10^{-18}	3.31×10^{-18}

Figure 10 compares the thermal and fast neutron spectra at the first measurement position (#1) and at fourth position (#4) calculated by the different methods. The neutron energy of interest in this benchmark includes both fast neutrons and thermal neutrons; therefore, the up-scattering effect in the thermal groups cannot be neglected. For neutrons with high energy, the angular fluxes in fast groups tend to be the most irregular or peaky, whereas anisotropy focuses on similar angular regions in various energy groups. As neutrons slow down, thermal fluxes become increasingly isotropic. Even homogenous lower-order quadrature sets with fewer directions can precisely integrate angular fluxes. The results of the traditional S_N calculation show a degree of overestimation, and the energy spectrum of the detector near the duct tail shows an unphysical drop at approximately 0.4 eV. The source iteration scheme for up-scattering is to add additional thermal iterations, and the decrease in the thermal energy region energy spectrum at 0.4 eV is largely due to the underestimation of the neutron flux due to insufficient angular directions for the thermal iteration. On the other hand, the results of the GO-MCS calculation are in agreement with the reference results, which shows that this algorithm can effectively control the angular discretization error of the traditional S_N calculation.

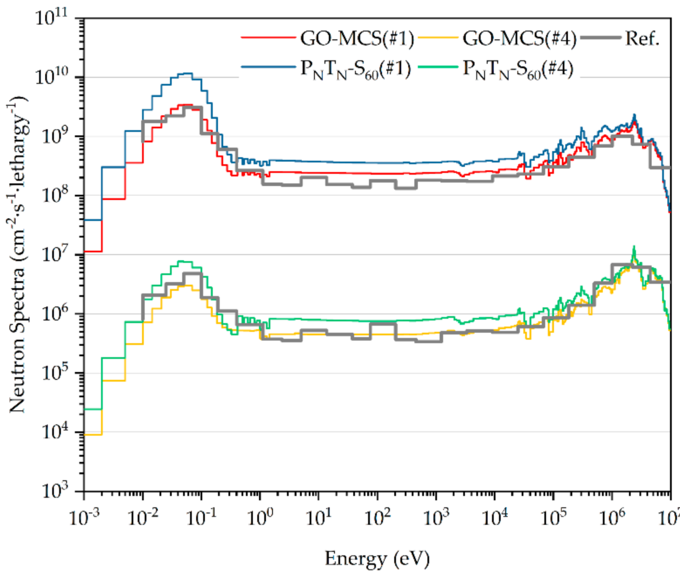

Figure 10. Neutron spectrum for the IRI-TUB benchmark.

Figure 11 depicts the quadrature set calls which are utilized in the GO-MCS computation as well as the time required for each quadrature set to complete one transport sweep. The numbers of calls for the six quadrature sets are 398, 640, 659, 586, 345, and 208, and the corresponding times needed for each transport sweep are 538 s, 264 s, 178 s, 118 s, 45 s, and 22 s, respectively. The total number of iterations for the P_NT_N-S_{60} calculation is approximately the same as the number of iterations for the GO-MCS calculation: 2853. The speedup of GO-MCS relative to the traditional S_N computation is approximately 1.28 for this problem. The GO-MCS method is verified to have acceptable accuracy for large and complex model neutron flow shielding problems through comparative calculations.

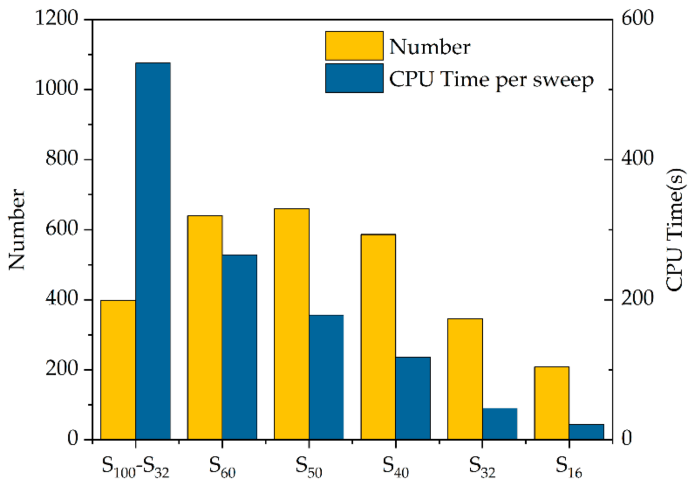

Figure 11. The number of times the quadrature is used for the IRI-TUB benchmark.

5. Conclusions

The purpose of this study was to demonstrate the capabilities of the GO-MCS algorithm module which is based on the multi-dimensional S_N transport program ARES for solving actual multigroup neutron streaming shielding problems. The IRI-TUB benchmark of SINBAD database was used to test the algorithm and compare the results obtained against the measured solutions. The GO-MCS method, in general, was found to provide reactive rates and neutron spectra that were determined to be in good agreement with the reference results.

For strong anisotropy of the angular flux in the neutron streaming problems, the GO-MCS algorithm uses spatial decomposition based on the contribution factor and dynamic quadrature technique to adaptively determine the partitioning of the geometry and dynamically change the angular quadrature order in the remaining iterations. In addition, the source iteration is modified to add thermal iteration for the up-scattering of thermal neutrons in actual reactor problems. Numerical results through detailed quantitative analysis indicate that the GO-MCS method produces a more efficient arrangement of angular quadrature sets for a given accuracy compared with uniform sets. In the self-designed simplified model, the goal-oriented method exhibits the same accuracy with a speedup of approximately 2 compared with the standard S_N calculation. For more difficult multi-group problems, our method also outperforms the standard S_N with a similar number of iterations. The results show that the goal-oriented collision source algorithm can effectively control the angular discretization error and reduce the scale of unknown quantities in the shielding calculation, which has better economy than the traditional discrete ordinates calculation.

Although the results presented here are illuminating, more comparisons with practical benchmarks are necessary to fully demonstrate the effectiveness of our method. Moreover, the method of quadrature error based on scalar fluxes is not efficient enough for the dynamic quadrature technique. Future studies will concentrate on the parallel technique and expand the goal-oriented multi-collision source method to numerous complicated transport problems.

Author Contributions: Conceptualization, X.W.; methodology, X.W.; software, X.W.; validation, X.W.; formal analysis, X.W.; investigation, J.X.; data curation, J.X.; writing—original draft preparation, X.W.; writing—review and editing, B.Z.; supervision, Y.C.; project administration, Y.C.; funding acquisition, B.Z. All authors have read and agreed to the published version of the manuscript.

Funding: This research was funded by National Natural Science Foundation of China: 11975097.

Data Availability Statement: Not applicable.

Conflicts of Interest: The authors declare no conflict of interest.

References

1. Lewis, E.; Miller, W. *Computational Methods of Neutron Transport*; Wiley: Hoboken, NJ, USA, 1984.
2. Lathrop, K. Ray effects in discrete ordinates equations. *Nucl. Sci. Eng.* **1968**, *32*, 357–369. [CrossRef]
3. Lathrop, K.; Carlson, B. *Discrete Angular Quadrature of the Neutron Transport Equation*; Report LA-3186; Los Alamos Scientific Laboratory: Los Alamos, NM, USA, 1965.
4. Cacuci, D. *Handbook of Nuclear Engineering*; Springer: New York, NY, USA, 2010.
5. Lathrop, K. Remedies for Ray Effects. *Nucl. Sci. Eng.* **1971**, *45*, 255–268. [CrossRef]
6. Compton, J.; Clouse, C. *Domain Decomposition and Load Balancing in the AMTRAN Neutron Transport Code*; Report UCRL-JC-152231; Lawrence Livermore National Laboratory: Los Alamos, NM, USA, 2003.
7. Longoni, G.; Haghighat, A. Development of New Quadrature Sets with the 'Ordinate Splitting' Technique. In Proceedings of the ANS International Meeting on Mathematical Methods for Nuclear Applications, Salt Lake City, UT, USA, 9–13 September 2001.
8. Longoni, G.; Haghighat, A. Development and Application of the Regional Angular Refinement Technique and its Application to Non-Conventional Problems. In Proceedings of the PHYSOR 2002 ANS Topical Meeting, Seoul, Korea, 7–10 October 2002.
9. Sjoden, G.; Haghighat, A. *PENTRAN: A Three-Dimensional Scalable Transport Code with Complete Phase-Space Decomposition*; Transactions of the American Nuclear Society: Reno, NV, USA, 1996.
10. Alcouffe, R.; O'Dell, R.; Brinkley, F. A First-collision Source Method That Satisfies Discrete Sn Transport Balance. *Nucl. Sci. Eng.* **1990**, *105*, 198–203. [CrossRef]
11. Childs, R.; Pace, J. *GRTUNCL: An Analytic First Collision Source Code*; Oak Ridge National Laboratory: Oak Ridge, TN, USA, 1992.

12. Konno, C. TORT Solutions with FNSUNCL3 for Kobayashi's 3D Benchmarks. *Prog. Nucl. Energy* **2001**, *39*, 167–179. [CrossRef]
13. Evans, T.M.; Stafford, A.S.; Slaybaugh, R.N.; Clarno, K.T. Denovo: A new three-dimensional parallel discrete ordinates code in SCALE. *Nucl. Technol.* **2010**, *171*, 171–200. [CrossRef]
14. Zmijarevic, I. Multidimensional discrete ordinates nodal and characteristics methods for APOLLO2 code. In Proceedings of the International Conference on Mathematics and Computation, Reactor Physics and Environmental Analysis in Nuclear Application, Madrid, Spain, 27–30 September 1999.
15. Kim, J.W.; Lee, C.W.; Lee, Y.O.; Lee, D.W.; Cho, S. Development of discrete ordinates code supporting unstructured tetrahedral mesh and applied in neutronics analysis for the Korea helium cooled ceramic reflector test blanket module. *Fusion Eng. Des.* **2014**, *89*, 1172–1176. [CrossRef]
16. Chen, Y.; Zhang, B.; Zhang, L.; Zheng, J.; Zheng, Y.; Liu, C. ARES: A parallel discrete ordinates transport code for radiation shielding applications and reactor physics analysis. *Sci. Technol. Nucl. Ins.* **2017**, *2017*, 2596727. [CrossRef]
17. Wang, X.; Zhang, B.; Chen, Y. Goal-oriented multi-collision source algorithm for discrete ordinates transport calculation. *Nucl. Eng. Technol.* **2022**, *54*, 2625–2634.
18. Squires, G. *Introduction to the Theory of Thermal Neutron Scattering*; Dover Publication: New York, NY, USA, 1978.
19. Stamm'ler, R.; Abbate, M. *Methods of Steady-State Reactor Physics in Nuclear Design*, 2nd ed.; Academic Press: San Diego, CA, USA, 1988.
20. Williams, M. Generalized Contributon Response Theory. *Nucl. Sci. Eng.* **1991**, *108*, 355–383. [CrossRef]
21. Kloosterman, J.; Hoogenboom, J.; Zsolnay, E. Experiments and calculations on neutron streaming through bent ducts. *Nucl. Sci. Technol.* **1993**, *30*, 611–627. [CrossRef]
22. Kim, D.; Gil, C.; Lee, Y. Validation of an ENDF/B-VII.0-based neutron and photon shielding library in MATXS-format. *Korean Phys. Soc.* **2011**, *59*, 1199–1202. [CrossRef]
23. Nelkin, M. Scattering of Slow Neutrons by Water. *Phys. Rev.* **1960**, *119*, 741–746. [CrossRef]
24. Parks, D.; Beyster, J.R.; Wikner, N.F. Thermal Neutron Spectra in Graphite. *Nucl. Sci. Eng.* **1962**, *13*, 306–324. [CrossRef]